Direct Force Measurements of Specific and Nonspecific Protein Interactions†

D. E. Leckband,*,‡ F.-J. Schmitt,§ J. N. Israelachvili,§ and W. Knoll∥

Department of Chemical Engineering, State University of New York at Buffalo, Buffalo, New York 14260, Department of Chemical Engineering, University of California, Santa Barbara, California 93106, and Max-Planck-Institut für Polymerforschung, Ackermannweg 10, D-55021 Mainz, Germany

Received May 12, 1993; Revised Manuscript Received February 16, 1994®

ABSTRACT: Streptavidin–biotin (receptor–ligand) interaction forces were measured directly as a function of their intermolecular separation in various salt solutions and at various temperatures with a surface forces apparatus. Electrostatic and van der Waals forces were found to dominate the long-range streptavidin–biotin interaction at >20 Å. At intermediate separations, down to ~10 Å, the interaction is governed by repulsive steric and attractive van der Waals and hydrophobic forces. A much stronger short-range attraction giving rise to the strong, specific adhesive binding was measured at molecular separations of less than 5 Å. A decrease in the pH from 7.2 to 6.0 resulted in complete charge reversal on the binding surface of streptavidin ($pK \sim 6$) from net negative to net positive, while leaving the negatively charged biotin surface ($pK \sim 3.0$) unchanged, and the long-range interaction switched from repulsive to attractive. This observed behavior can be attributed to the titration of two histidines on the biotin binding surface of streptavidin. These results reveal a strong sensitivity of the long-range interaction forces to the detailed amino acid composition of the biotin binding surface. They also demonstrate the powerful regulatory potential conferred by small changes in local surface ionic conditions on protein interaction forces over different distance regimes. The effects of temperature on receptor–ligand dynamics and on the strength of intermembrane adhesion forces were studied by measuring the long-range force profiles and short-range adhesion forces above and below the chain melting temperature ($T_c \sim 30$ °C) of the lipids in the supporting bilayers. Increased bilayer fluidity due to a temperature increase to 33 °C ($T > T_c$) increased short-range adhesion by 7-fold relative to bilayers in the gel state at 25 °C ($T < T_c$). This effect was attributed to the enhanced rates of lateral diffusion and molecular rearrangements on the more fluid bilayer surfaces, which resulted in greater and more rapid intermembrane bond formation. A change in the rates of molecular rearrangements was also found to affect the repulsive part of the interaction potential at intermediate separations (10–20 Å) via modulation of the steric repulsion between streptavidin and the highly flexible, polymer-like biotin molecules. This is expected to have a large effect on the association rates of receptor–ligand binding, even if it does not change the equilibrium binding energy. These results indicate that the lateral mobility of receptors and the flexibility of protruding ligand groups are also important determinants of the effective strength of specific intermembrane adhesion.

The high selectivity of biological interactions results from the combined action of nonspecific electrostatic, van der Waals, steric, and hydrophobic forces, as well as short-range hydrogen bonds. The interactions deduced from crystallographic and NMR studies, as well as by chemical modification and genetic manipulation, verified the role of short-range forces in biological recognition (Creighton, 1989). Forces such as electrostatic (double layer), van der Waals, and hydrophobic interactions between two surfaces, however, may extend to separations greater than 100 Å (Israelachvili, 1991; Israelachvili & Pashley, 1982; Claesson et al., 1990). These forces are all operative in biological recognition, which suggests that the interaction potential may extend beyond the immediate region of the protein binding site. Furthermore, although equilibrium binding constants are often interpreted solely in terms of contact interactions, longer ranged forces contribute to the measured constants (Baltz & Cone, 1990). Long-range forces, which purportedly orient bimolecular trajectories, are frequently invoked to account for reaction rates exceeding the diffusion-controlled limit (Wendolowski et al., 1987; Northrup et al., 1988; Margoliash & Bosshard, 1983; Creighton, 1989).

Brownian dynamics simulations demonstrated that enzyme–substrate and interprotein charge complementarity can enhance association rates by as much as 30-fold (Sharp et al., 1987a; Allison et al., 1985; Northrup et al., 1988). Similarly, cytochrome P-450 mutants with altered surface charge near the active site exhibit reduced donor binding constants and electron-transfer reaction rates (Stayton & Sligar, 1990). The electric field of a protein may also influence enzymatic activity, presumably by preorienting approaching ligands (Koppenol & Margoliash, 1982; Matthew et al., 1983; Wendoloski et al., 1987; Northrup et al., 1987, 1988). The latter results provided strong evidence that enhanced molecular collision rates are due to attractive, possibly long-range, intermolecular forces that lower the association activation barrier. While the existence of such mechanisms is generally accepted, the origin and mode of action of the corresponding attractive forces have yet to be verified by direct experimental measurements. Some studies suggest an electrostatic origin (Matthew et al., 1983; Wendoloski et al., 1987; Northrup et al., 1987, 1988; Koczak & Subramanian, 1993), whereas direct force measurements between model membrane systems suggest that long-range hydrophobic forces may also be involved, possibly triggered

† This work was supported by the NIH (PHS GM77334) and the NSF (BCS-9310014). D.E.L. was an NIH postdoctoral fellow (PHS GM13300). F.J.S. was supported by a fellowship from the Deutsche Forschungsgemeinschaft.

* Author to whom correspondence should be addressed.
‡ State University of New York at Buffalo.
§ University of California at Santa Barbara.
∥ Max-Planck-Institut für Polymerforschung.

® Abstract published in *Advance ACS Abstracts,* April 1, 1994.

0006-2960/94/0433-4611$04.50/0

by a change in the ionic binding at the surfaces (Leckband et al., 1992, 1993). It is possible that electrostatic and hydrophobic forces act synergistically, and one of the aims of the present study was to identify and quantify the different contributions made by long-range electrostatic, van der Waals, and hydrophobic forces to the receptor–ligand interaction potential.

In cell adhesion models, receptor-mediated cell adhesion strength depends strongly on lateral receptor mobility, as well as on the strength of discrete receptor–ligand bonds (Bell, 1988; Bongrand & Bell, 1984; Torney et al., 1986; Lauffenburger, 1991). Cell surface receptor diffusivity has been well-characterized (Ryan et al., 1988; Roess et al., 1988). Additionally, increases in the cell adhesive strength corresponding to cell spreading and increased contact area has been quantified extensively (Evans et al., 1991; Evans, 1985). However, although the importance of surface dynamics and lateral rearrangements in cellular adhesion is generally accepted, the effect of lateral mobility modulation on intermembrane adhesion has never been measured quantitatively.

In this work, the forces and molecular mechanisms involved in specific intermolecular and intermembrane recognition have been measured directly with the surface forces apparatus. The model receptor–ligand system consisted of streptavidin and biotin anchored to opposing lipid bilayers (Leckband et al., 1992; Helm et al., 1991; Blankenburg et al., 1989; Darst et al., 1991). Both the long-range and short-range specific streptavidin–biotin interaction forces were measured directly as a function of the intersurface (membrane–membrane) separation, D.

The effects of lateral mobility and molecular rearrangements on the ligand–receptor-mediated intermembrane adhesion were examined at two different temperatures, above and below the solid–liquid transition temperature, T_c = 30 °C, of the lipids in the bilayer (Cevc, 1987). At 33 °C, one expects that the streptavidin and biotin molecules can diffuse freely in the bilayer, mutually realigning to facilitate bond formation and allowing the maximum number of bonds to form within a given time. In contrast, at 25 °C, the lateral mobilities of the surface molecules are expected to be restricted by the reduced membrane fluidity, so that mismatches in receptor–ligand orientations and positions on opposing surfaces are not rapidly relieved, resulting in fewer intermembrane bonds and consequently lower adhesion. Intermembrane binding strength was also measured as a function of the biotin surface concentration, with both fluid and frozen bilayers. Binding strengths were measured at two biotin coverages, which differed by an order of magnitude.

These results present a detailed description of the full interaction potential for this receptor–ligand system, ranging from $D > 500$ Å to intermolecular contact within ~1-Å resolution. The resulting potential is demonstrated to be a superposition of at least three and possibly four different types of intermolecular forces (van der Waals, electrostatic, steric, and hydrophobic), each operating with a different magnitude over different length scales and subject to different surface and solution conditions. The detailed distance dependencies of these constituent forces and their sensitivities to solution conditions facilitated measurements of the strength of adhesion and of the long-range forces that determine kinetic association rates under different solution conditions. The net interaction is modulated by variations in the constituent forces, so that the resulting interaction potential may be attractive and repulsive over different distance regimes. It is most likely that biological regulation results from the selective modulation of such forces *in vivo*.

MATERIALS AND METHODS

Materials. *N*-[6-(Biotinylamino)hexanoyl]dipalmitoyl-L-α-phosphatidylethanolamine (biotin-X-DPPE) was purchased from Molecular Probes. Dipalmitoylphosphatidylethanolamine (DPPE) and dilaurylphosphatidylethanolamine (DLPE) were purchased from Avanti Polar Lipids. Polysulfone Acrodisc filters were purchased from Gelman. Streptavidin (Bayer & Wilchek, 1990) was either obtained as a gift from Boehringer-Mannheim (Werk Tützing) or purchased from Calbiochem. Biotin was from Calbiochem. NaH_2PO_4 and Na_2HPO_4 (at least 99.95% purity) were purchased from Aldrich, and NaCl was from Fluka. All water was doubly distilled and filtered through a Millipore Ultrapure system prior to use. Prior to filling the chamber of the apparatus, the DLPE-saturated phosphate buffer was filtered through a 0.2-μm Durapore membrane (Millipore) to remove particulates, lipid aggregates, and microbes. All solutions were stored in NoChromix-treated (Aldrich) glassware.

Force Measurements. Force measurements were made with a surface forces apparatus described elsewhere (Marra & Israelachvili, 1985). The apparatus spectrometer was interfaced with a video camera recorder system equipped with a video micrometer and an internal timer (Israelachvili, 1992). In some measurements, the intersurface forces were determined by the drainage method (Chan & Horn, 1986).

The measurements were carried out at 25 °C or 33 °C. Prior to each experiment, the apparatus was equilibrated with a 0.1 mM NaCl solution at pH 6 or a solution of 0.05 mM NaH_2PO_4 and 0.08 mM Na_2HPO_4 at pH 7.2. In all cases, the solution was saturated with DLPE to prevent DLPE desorption from the bilayers during an experiment (Marra & Israelachvili, 1985). In cases where the ionic strength was increased during an experiment, 10 mL of 3.5 M $NaNO_3$ in 0.1 mM phosphate buffer was added to give a final $NaNO_3$ concentration of 0.01 M.

The forces measured during the initial interactions between the two surfaces were determined by the dynamic method, after the manner of Chan and Horn (1986). In these experiments, the surfaces are driven together at a constant driving velocity. The spring deflects under the combined influence of both hydrodynamic and intersurface forces, and the latter forces are determined by subtraction of the hydrodynamic force from the total measured force.

Preparation of Biotin-X-DPPE and Streptavidin Surfaces. A 5 mol % biotin-X-DPPE/95 mol % DLPE monolayer was spread at the air–water interface and compressed to an average molecular area of 60 ± 3 Å^2 at 25 °C on a 1 mM NaCl subphase, as described previously (Leckband et al., 1992; Schmitt et al., 1992; Helm et al., 1991). The biotin–lipid monolayer was transferred at constant pressure onto a monolayer of DPPE (43 Å^2/molecule) deposited on mica, thereby forming a supported bilayer membrane. For simplicity, this will be referred to as the 5% biotin surface. In the absence of any further treatment, the sample was transferred underwater to the apparatus and mounted as described previously (Marra & Israelachvili, 1986). In some experiments, a 0.5% biotin-X-DPPE solution was used. The monolayer was compressed to the same mean molecular area of 60 ± 3 Å^2. This will be referred to as the 0.5% biotin surface.

Lyophilized streptavidin was dissolved in MilliQ water to yield a concentration of 1 mg/mL. Prior to adsorption, the streptavidin solution was centrifuged at 5000*g* for 30 min at

room temperature. This treatment rendered the solution free of aggregates and large particulates, as assessed by dynamic light scattering. The protein was adsorbed to the biotin-functionalized supported bilayers by two methods. When streptavidin was to be adsorbed to both opposing biotin surfaces, ~50 μL of the 10 μM solution of streptavidin was injected through a polysulfone Acrodisc 13 filter (Gelman), which was previously flushed with 15 mL of ultrapure water, into the apparatus directly between the two biotin surfaces. Prior to injection of the protein, the surfaces were separated by 3–4 mm. The streptavidin equilibrated with the biotin surfaces for 1–2 h at 25 °C prior to data acquisition.

When only one surface was modified by the streptavidin, one biotin surface was placed in 2.5 mL of a 10^{-7} M solution of streptavidin in 1 mM phosphate buffer at pH 7.2 and 25 °C for 2 h. Following the incubation, the sample was rinsed thoroughly with 600 mL of Durapore-membrane-filtered 1 mM phosphate buffer at pH 7.2 to remove nonspecifically bound streptavidin. The streptavidin surface was then mounted in the apparatus. The second surface was a biotin surface prepared as described above.

Theoretical Computation of DLVO Force Profiles between Asymmetric Surfaces. All measured force profiles were first compared to the theoretical DLVO force profile, which consists of the electrostatic double-layer force together with the van der Waals force. The double-layer forces were computed by solving the nonlinear Poisson–Boltzmann (NLPB) equation. The van der Waals forces were obtained by solving the full Lifshitz equation for retarded van der Waals forces, including the effect of ionic screening on the zero-frequency component of the interaction. In order to calculate the double-layer force between two dissimilar surfaces, each having a different surface charge or potential (or charge regulation mechanism), these parameters or boundary conditions must be specified independently for each surface when obtaining numerical solutions to the NLPB equation. Numerical solutions giving the double-layer force, with the computed van der Waals force added to obtain the full DLVO force law, were obtained with software generously provided by Grabbe (1993). In some cases, prior to fitting the experimental data, the biotin surface charge parameters, which had been determined previously (this work; Helm et al., 1991), were fixed, and the streptavidin surface parameters were allowed to vary.

RESULTS

Definition of Bilayer–Bilayer Contact and Measurement of Protein Layer Thickness. The separation distance defined as $D = 0$ Å corresponds to the equilibrium separation between two biotin–lipid surfaces in contact. The thickness of a single adsorbed streptavidin layer was determined from the thickness change following the adsorption of streptavidin to one biotin–lipid surface. The thickness of a single streptavidin monolayer was previously found to be 44 ± 1 Å (Leckband et al., 1992; Weber et al., 1992; Darst et al., 1991; Schmitt et al., 1992; Herron et al., 1992; Helm et al., 1991; Vaknin et al., 1991). In these experiments, the thickness of the bound streptavidin layer, measured with the optical technique of the surface forces apparatus, was 45 ± 2 Å, which is consistent with a single bound streptavidin monolayer. When streptavidin was bound to both surfaces, the first or primary attractive minimum measured following protein adsorption occurred at $D = 86$ Å, corresponding to two monolayers of streptavidin, at 43 Å per layer, between the bilayer surfaces.

In the experiments in which biotin–streptavidin force–distance profiles are measured, the separation distance D again refers to the distance between bilayer surfaces lacking protein. However, since the thickness of bound streptavidin is 45 Å, the biotin surface will contact the streptavidin surface at $D = 45$ Å. In this work, all interbilayer separations are reported in terms of the bilayer–bilayer separation, D, while the separation between the biotin and streptavidin surfaces are reported in terms of D_{BA} (where $D_{BA} = 0$ at $D = 45$ Å).

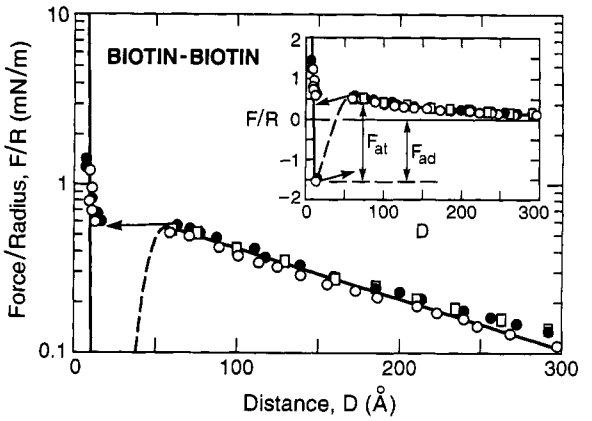

FIGURE 1: Measured force–distance profile between two 5% biotin surfaces in 0.1 mM salt at pH 6 and 25 °C ($T < T_c$). The long-range interaction at $D > 50$ Å is dominated by the electrostatic double-layer repulsion between the negatively charged groups on the biotin surface. Closer in, the van der Waals attraction dominates, pulling the surfaces into adhesive contact at $D = 8$ Å. The pull-off position from adhesive contact is indicated in the inset by the outward directed arrow. The results of three independent force measurements are shown by the different symbols: ○, ●, □.

Biotin–Biotin Interactions. A typical force curve describing the interaction between two 5% biotin–lipid surfaces is shown in Figure 1 (solution conditions: 0.1 mM NaCl, pH 6, T = 25 °C, *i.e.*, $T < T_c$). At pH 6, the biotin surface is negatively charged (pK ~ 3), and at long range the intermembrane interaction is dominated by the electrostatic double-layer force which, between two similarly charged surfaces, is exponentially repulsive. The measured exponential decay length of 167 ± 10 Å is consistent with the theoretical Debye length of λ_D = 172 Å, calculated from

$$\lambda_D = \kappa^{-1} = \sqrt{[\mathrm{NaCl}]e^2/\epsilon\epsilon_0 kT} \qquad (1)$$

where [NaCl] is the salt concentration in molecules/dm^3, e is the electronic charge, ϵ is the relative dielectric constant or permittivity of the liquid, ϵ_0 is the permittivity of free space, k is the Boltzmann constant, and T is the absolute temperature (Israelachvili, 1991).

The surface potential is determined directly from the force curve. For two double layers interacting at separations greater than 2–3 Debye lengths, the surface potential, ψ_0, is related to the double-layer force by the following approximate equation (Adams & Israelachvili, 1976; Hunter, 1989):

$$\psi_0 = \frac{4kT}{e}\left\{\tanh^{-1}\sqrt{\frac{F(D)\kappa \exp(\kappa D)}{128Rn\pi kT}}\right\} \qquad (2)$$

where n is the number density of monovalent counterions in the bulk solution. For the 5% biotin–lipid surface (Figure 1), the determined surface potential was $\psi_0 = 59 \pm 8$ mV. The surface charge density, σ, is obtained from the Grahame equation (Israelachvili, 1991):

$$\sigma^2 = 2\epsilon\epsilon_0 kT[\mathrm{NaCl}]\{2\sinh(e\psi_0/kT) - 2\} \qquad (3)$$

where σ is in units of C/m^2. The charge density was 5400

Table 1: Summary of the Double-Layer Properties of Biotin-Functionalized Bilayers

biotin surface (area per biotin, Å²)	temp (°C)	pH	surface potential, ψ_o (±5 mV)	surface charge (Å²/unit charge)	degree of ionization (%)
5% biotin	25	6	−59[a]	5400	22
	($T < T_c$)	7.2	−54	5500	22
(1200)	33	6	−60	3500	34
	($T > T_c$)	7.2	−59	1250	21
0.5% biotin	25				
	($T < T_c$)	7.2	−29	13000	92
(12 000)	33				
	($T > T_c$)	7.2	−28	13300	90

[a] Error: ±8 mV.

± 1000 Å² per unit charge. Since the biotin surface density is 1200 Å²/molecule, the degree of ionization is 1200/5400 or 0.22 ± 0.05. At pH 7.2, the surface potential is 54 ± 3 mV, corresponding to a charge density of 5500 Å² per unit charge, which shows that neither the surface charge nor the surface potential is affected in this pH range, which is as expected since p$K \approx 3$ for the phosphate groups on the biotin-X-DPPE lipid. These results are summarized in Table 1.

At smaller separations, $D < 50$ Å, the van der Waals force dominates, and the surfaces undergo an instability when the gradient of the force exceeds the spring constant. The two surfaces then rapidly snap together into an attractive minimum at $D = 8$ Å (see top arrow in the inset of Figure 1). The depth of the adhesive minimum is determined from the tensile force necessary to separate the surfaces, the pull-off or adhesion force, F_{ad}. The corresponding adhesion energy per unit area, E_{ad}, is obtained from the pull-off force normalized by the geometric averaged radius R of the two curved surfaces according to (Chen et al., 1991; Leckband et al., 1993)

$$E_{ad} = F_{ad}/3\pi R \quad (4)$$

The normalized adhesion force F_{ad}/R was 1.6 mN/m (Figure 1, inset), corresponding to an adhesion energy of 0.34 mJ/m². For the equivalent geometry of two interacting crossed cylinders, the nonretarded Hamaker constant, A, can be determined from the measured force curve from (Israelachvili, 1991)

$$A \approx 6F_{at}\Delta D^2/R \quad (5)$$

where F_{at} is the *total* attractive force at the position of the adhesive minimum (*cf.* Figure 1, inset), and ΔD is the distance of the adhesive minimum from the van der Waals plane of origin, D_{vdW}. The position corresponding to $D_{vdW} = 0$ was taken to be the same as $D = 0$ (dehydrated bilayer contact), so that $\Delta D = 8$ Å. The measured Hamaker constant was therefore $A = 1 \times 10^{-20}$ J, which is somewhat higher than expected for two pure hydrocarbon phases interacting across an aqueous gap (Marra & Israelachvili, 1985; Israelachvili, 1991).

Similarly, the measured force profiles between two 0.5% biotin surfaces at pH 7.2 and 25 °C ($T < T_c$) are shown in Figure 2. The force profiles are qualitatively and quantitatively similar to those measured between 5% biotin surfaces at 25 °C and pH 6. The double-layer decay length was 145 Å (*cf.* theoretical $\lambda_D = 153$ Å), and the calculated surface potential and surface charge density were $\psi_o = 29$ mV and 13 000 Å²/unit charge, respectively (Table 1). A 92% degree of ionization was calculated from the data at pH 7.2 (Table 1). From a separation of $D = 21$ Å, the surfaces jumped into adhesive contact at $D = 8$ Å, and the adhesive force F_{ad}/R was 1.23 mN/m, corresponding to $E_{ad} = 0.13$ mJ/m². The one notable contrast to the force curves obtained between 5% biotin–lipid at 25 °C was a steep increase in the repulsive force just before the jump at $D \approx 40$ Å (*cf.* Figure 2). This would be consistent with a double-layer force between surfaces interacting at constant surface charge density rather than at constant potential (Israelachvili, 1991; Marra, 1986).

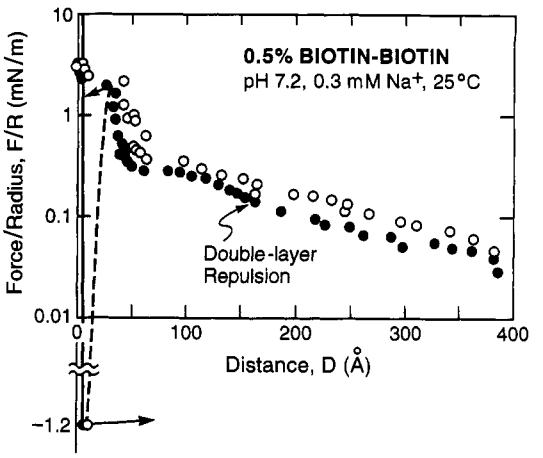

FIGURE 2: Force–distance profile between two 0.5% biotin surfaces in 0.3 mM salt at pH 7.2 and 25 °C. The results of two independent force measurements are shown by the different symbols: ○, ●.

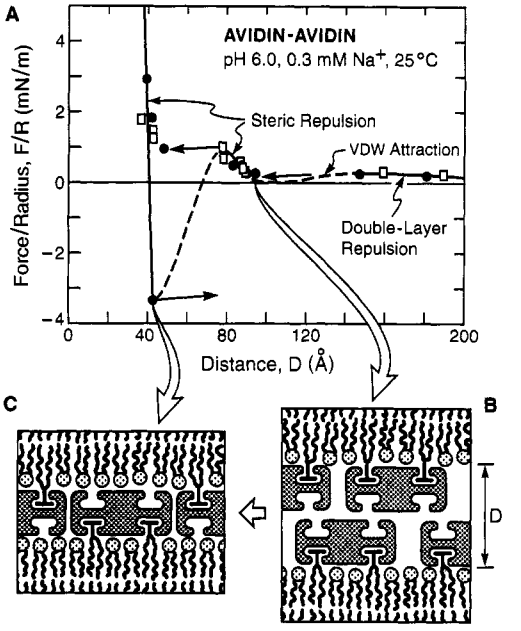

FIGURE 3: (A) Oscillatory force–distance profile between two streptavidin surfaces adsorbed to a 5% biotin surface in 0.3 mM salt at pH 6 and 25 °C. The results of two independent force measurements are shown by the different symbols: ●, □. (B, C) Proposed streptavidin–streptavidin interdigitation mechanism. Before interdigitation (B), the proteins occupy ~50% of the area of each surface. After interdigitation (C), the gap is ~100% occupied by protein.

Streptavidin–Streptavidin Interactions: Effect of pH. The isoelectric point (pI) of processed streptavidin is 6.0–6.5 (Green, 1975), and at pH 6, the net charge on streptavidin is positive. Figure 3A shows the force–distance curves for the interaction of two streptavidin surfaces in 0.1 mM NaCl at pH 6 and 25 °C ($T < T_c$). In contrast to previous studies on streptavidin interaction forces at 33 °C ($T > T_c$) (Helm et al., 1991), at 25 °C the proteins are expected to be less mobile on the bilayer surface. Figure 3A shows that, at large separations ($D > 150$ Å), the streptavidin interactions are dominated by a weak electrostatic double-layer repulsion with

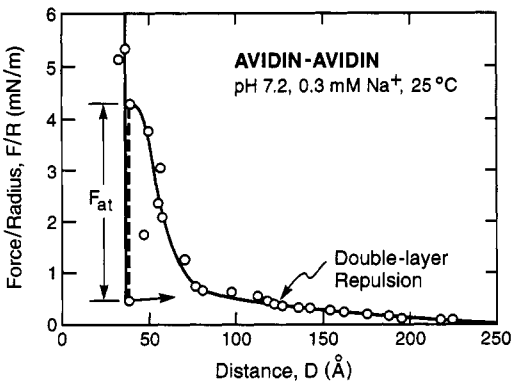

FIGURE 4: Force–distance profile between two streptavidin surfaces in 0.3 mM salt at pH 7.2 and 25 °C.

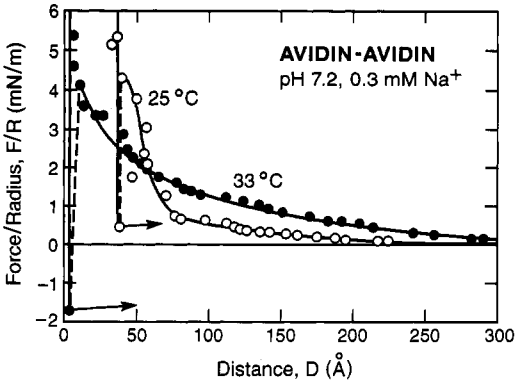

FIGURE 5: Force–distance profiles between two streptavidin surfaces in 0.3 mM salt at pH 7.2 measured above and below the lipid chain melting temperature: T_c = 30 °C.

a decay length of 158 Å (theoretical λ_D = 162 Å). The measured surface potential of the streptavidin surfaces is ψ_o = 29 ± 5 mV (assumed positive), corresponding to +0.5 unit charge per streptavidin. Since the double-layer force between two similar surfaces is repulsive regardless of the sign of the surface charge or potential, the sign of the protein charge cannot be determined.

Near D = 150 Å, the surfaces undergo an instability due to the interprotein van der Waals attractive force, and they jump into the outer adhesive (secondary) minimum at D = 86 Å. The position of this minimum corresponds to contact between two 43 Å thick protein monolayers, as illustrated in Figure 3B and consistent with previous studies (Leckband et al., 1992; Darst et al., 1991; Hendrickson et al., 1989; Helm et al., 1991; Weber et al., 1992). The measured net attractive force F_{at}/R between the two exposed surfaces of streptavidin is 0.8 mN/m.

Further compression results in a repulsive steric force as the protein layers overlap. Because the bilayer lipids are in the gel phase at 25 °C, the surface molecules cannot easily diffuse from the contact region to relieve the stress induced by the steric overlap. Some slight lateral mobility is possible, however, and the surfaces again jump from 75 Å into an inner (primary) adhesive minimum at D = 42 Å, corresponding to a single interdigitated monolayer of streptavidin between the lipid surfaces (Figure 3C) (Darst et al., 1991; Hendrickson et al., 1989; Helm et al., 1991; Weber et al., 1992). At 25 °C, the net attractive force at this position is F_{at}/R = 4.6 mN/m, about 6 times larger than at the outer minimum. However, the magnitude of this attraction is still consistent with a purely van der Waals interaction because of the significantly increased lateral protein contacts in the interdigitated state. By modeling the proteins roughly as rectangular solids with the same crystallographic dimensions (Weber et al., 1992), the protein–protein contact area is ~5 times greater in the interdigitated state, similar to the ~6-fold increase in the attractive force. The strong attractive force may also be due to closer lateral contacts in the interdigitated state, which would increase the van der Waals attraction, or due to hydrophobic interactions. The steep steric repulsion observed at D < 43 Å results from further compression of the proteins. Limited lateral mobility of the already crowded streptavidin surfaces prevents the proteins from diffusing out of the contact region in response to the externally applied force.

An increase in the pH from 6 to 7.2 (above the pI of streptavidin) is expected to change the sign of the streptavidin surface charge from net positive to net negative. The effect of the pH increase on the forces between two streptavidin surfaces is shown in Figure 4. The weak adhesive minimum at 86 Å, detected at pH 6, is now dominated by the stronger repulsive double-layer force and is therefore undetected, although a negative deviation in the otherwise exponentially repulsive force profile is evident at this separation. The magnitude of the attractive force $F_{at}/R \approx 4$ mN/m in the primary contact minimum at $D \approx 40$ Å apparently is unaffected.

If the outer Helmholtz plane is assumed to lie at D = 86 Å, the calculated surface potential and charge density of the exposed streptavidin surface at pH 7.2 are $\psi_o = |56| \pm 10$ mV (assumed negative) and 3400 Å^2/charge, respectively. Since the streptavidin surface coverage is ~5000 Å^2/streptavidin (Darst et al., 1991; Schmitt, 1991), the net unit charge per protein is 0.8 at pH 7.2. Again, the sign of the charge and surface potential cannot be determined from these measurements, although the streptavidin pI suggests that at pH 7.2 it is negative.

Effect of Temperature (Membrane Fluidity). Typically, contacts occur between biological membranes with exposed charged polysaccharides or membrane-bound proteins, and it was of interest to establish the mechanisms by which electrostatic and steric stresses arising from bilayer-associated biopolymers in the intermembrane gap might be relieved. In particular, we determined how the electrostatic, steric, and other forces between the exposed protein and biotin groups are affected by the fluidity of the supporting bilayers. Membrane fluidization was achieved by increasing the temperature from 25 °C, below the chain melting temperature T_c of the lipids, to 33 °C ($T > T_c$).

The effect of increased protein lateral mobility on the interactions is shown in Figure 5 (filled circles). For comparison, the force profile measured at 25 °C is indicated by the open circles. Although the force curves are similar to those measured between charged protein surfaces, in this case the intersurface separation was easily decreased to near interbilayer contact at $D \approx 0$. This can occur only if the proteins readily diffuse out of the contact region in response to the stresses in the gap. An adhesion of −1.8 mN/m was measured at $D \approx 0$, corresponding to a net attractive force of F_{at} = −5.7 mN/m, which is significantly larger than the expected van der Waals force of ~1–2 mN/m for fluid neutral bilayers at contact (Marra & Israelachvili, 1985). The magnitude of the attractive force could not be determined accurately, however, due to a complication from the additional nonequilibrium steric force arising from protein interactions; consequently, the true magnitude of the equilibrium attractive force is probably smaller than that indicated in Figure 5.

At 33 °C, the decay length of the measured repulsive force over the entire interaction range is longer than at 25 °C. The

magnitude of the double-layer force depends on the surface potential (Hunter, 1989; Israelachvili, 1991). As the two surfaces approach, the surface potential will decrease as charged proteins leave the contact region. This would reduce the double-layer repulsion at smaller distances, resulting in an apparent *increase* in the decay length, as observed (Figure 5). Protein diffusion is time-dependent; consequently, if the compression rate is faster than the streptavidin diffusion rate, a steric repulsive force would occur due to interactions between trapped proteins. This was verified in a rapid compression experiment conducted at 33 °C. A large steric repulsion was measured at 85 Å, the separation at which the streptavidin molecules begin to strongly overlap. The bilayer surfaces could not be brought into contact at this point due to the kinetically trapped protein molecules remaining in the gap. The similarity of the streptavidin interactions at pH 6 and 25 °C (Figure 3) to previous measurements at pH 6 and 33 °C (Helm et al., 1991) suggests that, in the absence of electrostatic repulsive forces, the proteins do not diffuse from the contact region.

The magnitude of the first steric barrier at $D \approx 86$ Å preceding protein interdigitation is only slightly higher at 25 °C (1 mN/m) than at 33 °C (~0.6 mN/m) (Helm et al., 1991). This indicates that the force necessary to induce the lateral redistribution of streptavidin and facilitate interdigitation is not significantly reduced by the bilayer fluidity. These observations suggest that the diffusivities in these systems are nearly equally slow on fluid or frozen bilayers, consistent with reports by Ryan et al. (1988) that receptor movement on crowded membrane surfaces is severely restricted.

Streptavidin–Biotin Interactions: Effect of Biotin Coverage. The 10^{15} M^{-1} streptavidin–biotin binding affinity is one of the strongest noncovalent interactions known (Green, 1975). The strong adhesion between streptavidin and biotin surfaces previously measured with the surface forces apparatus was consistent with this strong, specific affinity (Helm et al., 1991; Leckband et al., 1992). Since the reported short-range (D_{BA} < 10 Å) adhesion is due to the specific streptavidin–biotin interactions, the magnitude of the measured adhesion force strongly depends on the number of intermembrane attachments formed. Cell adhesion models predict that the adhesion varies linearly with the number of intermembrane bonds (Lauffenburger, 1991; Evans et al., 1991). Consequently, similar behavior is expected for streptavidin–biotin-mediated bilayer adhesion. In contrast, the general shape of the force law should be correspondingly independent of the number of intermembrane bonds (*i.e.*, the biotin and/or streptavidin surface densities).

Streptavidin–biotin interaction profiles were measured at pH 7.2 in 0.1 mM phosphate buffer (0.1 mM total phosphate). Two systems were examined. In the first, streptavidin was adsorbed to a 5% biotin surface. This yields an area of ~5000 Å²/streptavidin (Darst et al., 1991; Schmitt, 1991). The interactions of the streptavidin with (i) an opposing 5% biotin-lipid surface (1200 Å²/biotin) and (ii) an opposing 0.5% biotin–lipid surface (12 000 Å²/biotin) were then measured. Thus, the effect of a 10-fold reduction in the biotin surface density was examined at constant protein coverage. In the second system, streptavidin was immobilized to a 0.5% biotin–lipid layer (~50 000 Å²/streptavidin), and the interaction with an opposing 0.5% biotin–lipid layer (12 000 Å²/biotin) was examined. An illustration of the surface geometry corresponding to these receptor–ligand interactions is shown in Figure 6B.

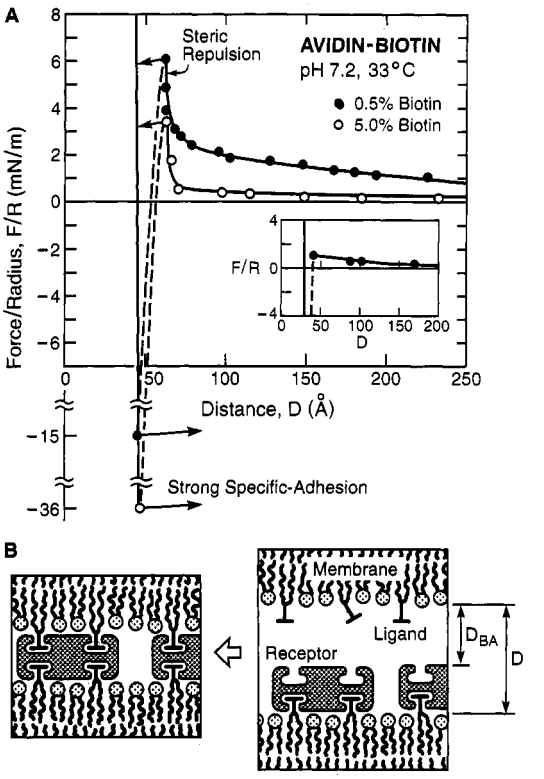

FIGURE 6: (A) Measured force–distance profiles for a streptavidin surface interacting with a 5% biotin surface (○) and a 0.5% biotin surface (●) in 0.3 mM salt at pH 7.2 and 33 °C ($T > T_c$). At this temperature, the outer monolayers are in the fluid state. The equilibrium force–distance profile, demonstrating the absence of the time-dependent steric force barrier at $D \approx 65$ Å ($D_{BA} \approx 20$ Å), is shown in the inset. (B) Schematic illustration of the biotin and streptavidin molecular configurations during their approach into strong adhesive contact at $D = 45$ Å ($D_{BA} = 0$ Å).

Figure 6A shows the force–distance profile for the interaction of a streptavidin surface at 5000 Å²/streptavidin with both 5% and 0.5% biotin surfaces. These experiments were conducted at pH 7.2 (>p*I*) and 33 °C. Both the streptavidin and biotin surfaces are presumably negatively charged, accounting for the dominance of a long-range electrostatic repulsive force at $D > 65$ Å ($D_{BA} > 20$ Å). The measured Debye lengths obtained with the 5% and 0.5% biotin–lipid surfaces were 105 and 112 Å, respectively. These are lower than the theoretical decay length of 135 Å, but similar to other decay lengths measured with streptavidin surfaces at this buffer composition (*cf.* Figures 3 and 4); consequently, the discrepancy may be due to weighing errors during the buffer preparation.

At separations of less than 55 Å ($D_{BA} < 10$ Å), the surfaces jump into strong adhesive contact under the influence of the strong, specific short-range attractive force. These jumps occurred from 55 Å, independent of the biotin surface coverage. The depths of the attractive forces giving rise to the jumps were determined from the force necessary to separate the surfaces. As shown in Figure 6, the intersurface adhesive forces were $F_{ad}/R = -38 \pm 4$ and -15 ± 4 mN/m when measured with 5% and 0.5% biotin surfaces, respectively. After a 30-min incubation with a 5% biotin surface, the adhesion increased by 20%, indicative of further diffusion of unbound molecules into the contact region. At 5% biotin coverage, the biotin concentration exceeds the streptavidin binding site density by 2.3. If we assume that at 5 mol % biotin all streptavidin sites bind biotin within 5–10 min (the measurement time), a 10-fold reduction in the biotin concentration is expected to reduce the adhesion to 0.1 × 2.3, or 23% of the

value at 5%. That is, the adhesion force should drop to 0.23 × 35 ≈ 8 mN/m. The measured value of −15 mN/m is about 60% lower, which is outside the limits of experimental error. However, higher adhesion is not unexpected since biotin diffusion at 33 °C should allow new biotin-lipid molecules to diffuse into the contact area with time. Indeed, after a sufficiently long time in contact, the adhesive force should rise to the same maximum value as was measured with the 5% biotin surface.

When the forces were remeasured immediately after surface separation, the short-range adhesion typically decreased by an order of magnitude, and a steep steric repulsive force was measured at $D < 70$ Å ($D_{BA} < 25$ Å). These observations suggest that surface damage occurs upon separation of the tightly adhering membranes (Helm et al., 1991). Damage presumably results from the cohesive failure of the bilayer rather than from the streptavidin–biotin bond fracture, resulting in nonbinding molecules whose outer surfaces now expose lipids that have been torn out of the opposing bilayer upon separation. Cell adhesion measurements exhibit identical behavior, in which high-affinity receptors are preferentially torn from the bilayer upon detachment of the adherent surfaces (Evans et al., 1991). In these experiments, the surfaces reanneal within 45–120 min, although >2 h are occasionally required for complete recovery of the initial adhesive force. During the reannealing period, the damaged proteins presumably diffuse out of the contact area into the reservoir of unaffected molecules and are replaced by unaffected streptavidin. This is substantiated by (i) the absence of the anomalous steric force after sufficient pauses between measurements (Helm et al., 1991; Leckband et al., 1992) and (ii) the complete recovery of the initial adhesion after a sufficient (45 min to 2 h) reannealing period. Thus, damaged molecules diffuse from the contact region, after which the contact area is replenished with unaffected molecules. Since the bilayers are in the fluid state at the temperature of the experiments, this result is as expected. The estimated diffusion constant over the sampled area of $\pi r^2 \sim 10\ \mu m^2$, is $D \sim r^2/t \approx 10^{-10}$–$10^{-11}$ cm^2/s, consistent with previous force measurements (Helm et al., 1991) and determined receptor diffusivities on cell surfaces (Barisas, 1984; Kapitza & Sackmann, 1980).

At small separations ($D < 65$ Å, $D_{BA} < 20$ Å), two types of interactions are evident, depending on the rate at which the surfaces are brought together. If the approach is rapid (>10 Å/s), a short-range, nonequilibrium steric force is measured at $D < 65$ Å (Figure 6). At 33 °C ($T > T_c$), the lipids are in a fluid state, and the membrane-associated biotin and streptavidin molecules diffuse freely over the surface. This short-range steric force occurs at $D_{BA} = 18 \pm 2$ Å, a separation identical to the length of the biotin moiety (Metzler, 1977), and is therefore attributed to nonequilibrium steric interactions between the biotin headgroups and the streptavidin surface. The opposing molecules are not initially aligned, and the biotin headgroups undergo a configurational search for the bound equilibrium orientation. In contrast, at slower rates of approach (<10 Å/s), the opposing biotin and streptavidin have sufficient time to rearrange and align before contact. In the latter case, the force profile lacks the steep repulsive barrier at $D_{BA} \approx 18$ Å, but the long-range repulsion and strong short-range attraction are unchanged (Figure 6, inset). The time dependence of these rearrangements is directly measurable. If the surfaces are rapidly brought to $D = 65$ Å ($D_{BA} = 20$ Å), the steric barrier collapses once the rearrangements occur and the surfaces jump into strong adhesive contact. The length of time before the jump indicates the relaxation time of the

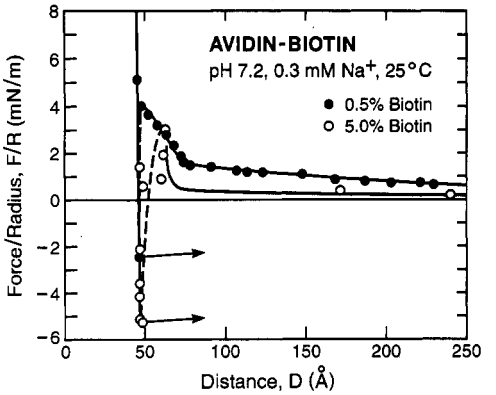

FIGURE 7: (A) Measured force–distance profiles for a streptavidin surface interacting with a 5% biotin surface (○) and a 0.5% biotin surface (●) in 0.3 mM salt at pH 7.2 and 25 °C ($T < T_c$). At this temperature, the outer monolayers are in the gel state.

reorientations, and in these experiments, the steric barrier collapses within 15 s. The proper orientation is therefore achieved within 15 s over a contact region of ~10 μm^2.

Effect of the Lipid Fluidity on Receptor-Mediated Intermembrane Adhesion. On fluid bilayers ($T > T_c$), streptavidin and biotin have limited surface mobility, and bond formation is facilitated by lateral diffusion and molecular reorientations during intermembrane contact, as described above. Conversely, if the lipids are in the solid or gel state, receptor–ligand mismatches on opposing membranes are frozen in. The restricted mobility prevents further molecular realignment and substantially reduces the number of intermembrane bonds formed. The result is a decrease in the intermembrane adhesion force. There is some lipid mobility in the gel state, and given sufficient time, the ligands and receptors would eventually adopt their equilibrium, bound configurations. However, on the time scale of these measurements (minutes, referring to the time in contact), at short equilibration times (<1 h), the measured adhesion between opposing frozen membranes bearing complementary ligands and receptors should be significantly reduced relative to that of fluid membranes.

In order to determine the effects of membrane fluidity on receptor-mediated intermembrane adhesive strength, the temperature of the experiment was reduced below the chain melting temperature to 25 °C. The streptavidin–biotin force–distance profiles obtained with 5% and 0.5% biotin surfaces at 25 °C and pH 7.2 are shown in Figure 7. At large separations, the force profiles are similar to those measured at 33 °C (*cf.* Figure 6). The restricted mobility, however, was manifested as two distinct, though related, effects. First, the short-range steric force was observed in these measurements, but its disappearance was not evident at 25 °C: namely, the steric force was always measured, regardless of the rate of approach of the two surfaces. This is attributed to the limited mobility at 25 °C, which prevents the molecular rearrangements on the time scale of the measurements. In contrast to the observed behavior at 33 °C, in order to move the surfaces into contact, additional force was applied in order to overcome the steric repulsion (Figure 7). Second, this lack of mobility was reflected further in the reduced adhesion relative to that measured at 33 °C under otherwise identical conditions. For example, with the 5% biotin surfaces, the adhesion is reduced to −6 ± 2 from −38 ± 4 mN/m at 33 °C. The adhesive force between streptavidin and 0.5% biotin surfaces was reduced from −15 ± 4 to only −2.5 ± 0.5 mN/m (Table 2). Thus, the molecular realignment, which results in strong adhesion, is also hindered. The temperature-dependent

Table 2: Intermembrane Adhesion

biotin surface (area per biotin, Å²)	streptavidin surface (area per streptavidin, Å²)	temp (°C)	adhesion force, F_{ad}/R (mN/m)
1200 (5%)	5000	25	−6 ± 2
		33	−38 ± 4
12 000 (0.5%)	5000	25	−2.5 ± 0.5
		33	−15 ± 4
1200 (5%)	50000	33	−2.2 ± 0.5

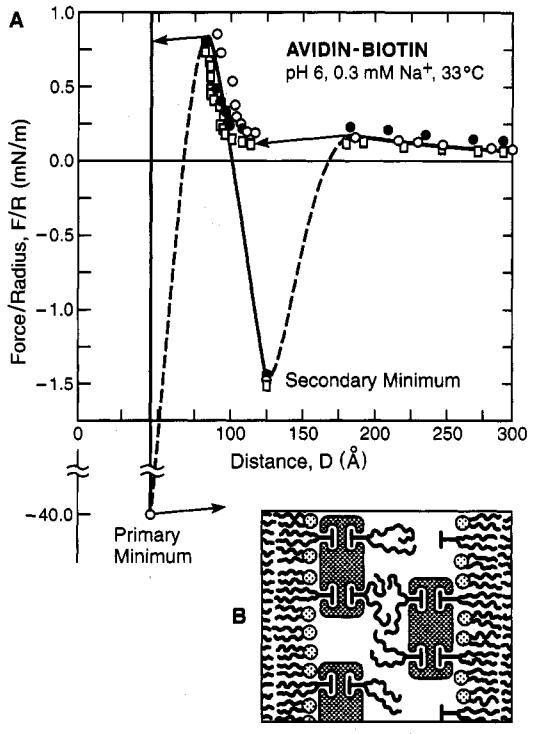

FIGURE 8: (A) Force–distance profiles between streptavidin and biotin surfaces, each supported on a DPPE monolayer with chains in the vertical crystalline configuration. In all previous force measurements, the chains of the supporting monolayers were in the tilted crystalline configuration. The results of three independent force measurements are shown by the different symbols: ○, ●, □. (B) Proposed molecular configuration of streptavidin molecules after pull-out.

mobility reduction is also evidenced by the observations that, following surface separation at 25 °C, (i) the apparent intermembrane contact was farther out by 20–40 Å, (ii) the adhesion dropped to <1 mN/m, and (iii) the damaged surfaces did not reanneal with time, in contrast with the observed behavior at 33 °C.

Influence of Epitaxial Coupling on Bilayer Fluidity. A consequence of the epitaxial coupling between the supporting or proximal DPPE monolayer and the distal or outer monolayers was observed when the phase state of the DPPE layer was altered. In the experiments described thus far, the proximal DPPE monolayer was deposited in the tilted crystalline phase. However, when the DPPE monolayer was deposited in the untilted crystalline phase, the fluidity in the distal layer was substantially reduced. When untilted DPPE supporting monolayers were used, the corresponding streptavidin–biotin force law measured >2 h after separation of the adherent surfaces at 33 °C is shown in Figure 8A. In contrast to force profiles measured on tilted crystalline DPPE layers (Figures 6 and 7 and later data in this work), Figure 8 exhibits two minima separated by a soft repulsive barrier. At large separations (D > 200 Å), the repulsive double-layer force dominates. From D = 195 Å (D_{BA} = 150 Å), the surfaces jump into the secondary minimum at 125 Å (D_{BA} = 80 Å). The jump-in begins slowly, accelerating as the surfaces approach the minimum. The adhesive force at 125 Å is −1.5 ± 0.2 mN/m, as determined from the pull-off force. Further compression results in a repulsive force, and from 90 Å the surfaces jump into the specific adhesive minimum at D = 45 Å (D_{BA} = 0 Å). The total attractive force at contact is −38 ± 4 mN/m.

The soft repulsive force at D < 100 Å is ascribed to steric interactions between streptavidin molecules now bound to both surfaces. Upon initial separation of the adherent surfaces, adhesive failure occurs within the bilayer membrane, and the biotin–lipid is pulled from membrane. Due to its 2-fold symmetry axis, streptavidin can be pulled to either surface (*cf.* Figure 8B). However, in contrast to the rapid reannealing observed on tilted crystalline DPPE layers, the pulled-out streptavidin clears from the contact region much more slowly. Upon recompression, proteins bound to the opposing surfaces make contact, resulting in the observed steric repulsion as well as a van der Waals attraction. Additionally, following separation from the primary minimum, the initial strong adhesive force recovered after 12 h, in sharp contrast to the ~1-h recovery observed with tilted DPPE proximal layers. In most cases, however, a weak residual steric repulsion at D = 90 Å was measured, indicating the presence of a small immobile fraction.

The determined molecular basis of the observed force law confirmed that damaged molecules diffuse out of the contact area much slower on vertical crystalline DPPE monolayers. The steric origin of the repulsive force at D < 100 Å was demonstrated by increasing the buffer concentration from 10^{-4} to 10^{-2} M total phosphate. The increased ionic strength reduces the decay length of the electrostatic force, while leaving nonelectrostatic forces, such as steric forces, unperturbed. The force curve measured at pH 6 in 0.01 M phosphate buffer at 33 °C is similar to that shown in Figure 8A. The double-layer force decays more rapidly (κ^{-1} = 30 Å), as expected. In contrast, the position of biotin–streptavidin contact is shifted out by 13 Å, and the magnitude of the short-range attractive force is reduced from −38 ± 4 to −15 mN/m. This reduction is attributed to steric repulsion due to hydrated ion binding at the surface (Marra, 1986; Claesson et al., 1989). The latter repulsion increases the distance of closest streptavidin–biotin approach and impedes complete binding. The steep repulsive force is still observed at D < 100 Å, consistent with its steric origin. The depth of the secondary minimum was ionic strength independent, substantiating the hypothesis that the secondary attractive minimum is due to interprotein van der Waals attraction and possible hydrophobic interactions between pulled-out lipids on opposing surfaces. Consequently, the slower diffusivity on vertical DPPE monolayers is demonstrated by the persistence of these damaged molecules in the contact region, in contrast to the behavior observed on tilted crystalline DPPE layers.

Determination of Streptavidin–Biotin Interaction Forces. Previous measurements of the forces between streptavidin- and biotin-coated surfaces suggested that the biotin–streptavidin interaction is influenced by the presence of an attractive force in addition to van der Waals and electrostatic forces (Leckband et al., 1992). In the present work, the constituent molecular forces operating in the recognition were determined by modeling the force curves as the superposition of the van der Waals and electrostatic double-layer forces (DLVO forces). Experimental deviations from the calculated DLVO forces would indicate the possible presence of non-DLVO

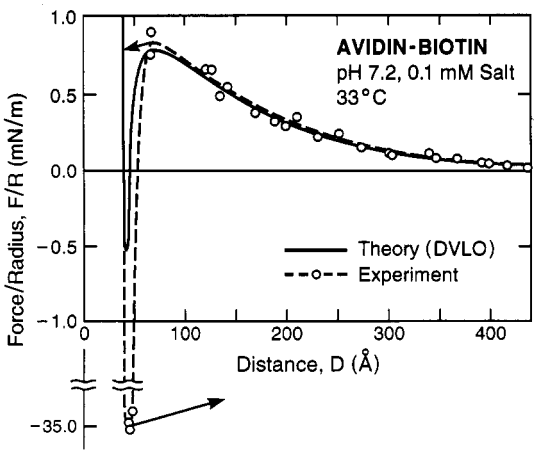

FIGURE 9: Measured force–distance profiles between a streptavidin surface and a 5% biotin surface in 0.1 mM salt at pH 7.2 and 33 °C ($T > T_c$). At this temperature, the outer monolayers are in the liquid state. The solid line represents the data fit to the theoretical DLVO force curve, with best fit parameters of $\Psi_S = -38 \pm 10$ mV and $\Psi_B = -55$ mV.

Table 3: Experimentally Determined Electrostatic Potentials of Biotin (B) and Streptavidin Surfaces (Active, S^+; inactive, S^-) Deduced from Fitting the Theoretical DLVO Force Function to the Measured Force–Distance Profiles[a]

	ψ_o (±5 mV)			ψ_o (±5 mV)	
pairs	pH 6	pH 7.2	pairs	pH 6	pH 7.2
B/B	−55/−55	−55/−55	S^-/S^-	nd	*−15[b]/−15[b]*
S^+/S^+	+29/+29	−51/−51	S^-/B	nd	*−38*/−47
S^+/B	+29/−55	−38[c]/−55			

[a] All DLVO fits were made using the experimentally determined Debye lengths, λ_D, which were generally within 10% of the theoretically expected values, and a Hamaker constant of $A = 10^{-22}$ J, including retardation and screening effects on the van der Waals forces (see text). All double-layer force fits were at constant potential except for potentials in italics. nd: not determined. [b] Error: ±2 mV. [c] Error: ±10 mV.

forces, such as hydrophobic forces. The theoretical fit to the data at pH 7.2 and 33 °C shown in Figure 9 (and Figure 10A) was obtained with the fitted potential of −55 mV for streptavidin and previously determined biotin surface potentials of 38 ± 10 mV (Table 3). The theoretical curve was calculated with a Hamaker constant of 10^{-22} J. In the latter fits, the biotin surface potential was fixed, and the streptavidin surface potential was allowed to vary. Charge regulation of both surfaces was controlled by constant surface potential. The good agreement between the determined streptavidin surface potential and that determined from force measurements between identical streptavidin surfaces (*cf.* Figure 3 and Table 3) suggests that the biotin–streptavidin interaction is governed entirely by DLVO forces. Additionally, fixing of the biotin surface boundary conditions facilitated determination of both the negative sign and magnitude (−38 mV) of the streptavidin potential.

Streptavidin was blocked (inactivated) with soluble biotin in order to demonstrate the specificity of the strong short-range adhesion. At pH 7.2, biotin inactivation increases the repulsive intersurface force at $D < 150$ Å ($D_{BA} < 105$ Å) (Figure 10B). The surface potentials and charge regulation behavior of the biotin-inactivated streptavidin at pH 7.2 were determined from theoretical fits to the data. The biotin surface potential but not the regulation behavior (boundary condition) was varied, while both the charge regulation mechanism and electrostatic potential of the biotin-inactivated streptavidin surface were allowed to vary. At pH 7.2, the data are described by two interacting charged surfaces: a biotin surface at a

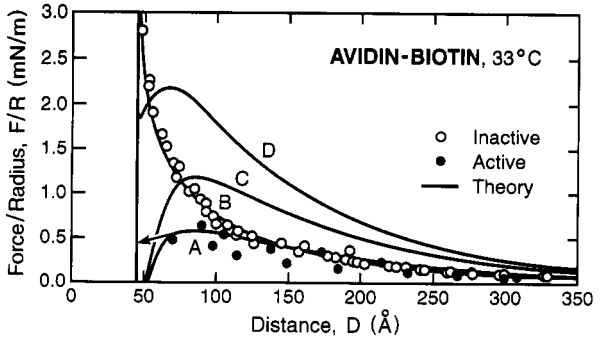

FIGURE 10: Force–distance profiles between a 5% biotin surface interacting with an active streptavidin surface (●) and a biotin-inactivated streptavidin surface (○) in 0.1 mM salt at pH 7.2 and 33 °C. The solid lines are theoretical DLVO force profiles at the specified salt composition, each computed for a Hamaker constant of $A = 10^{-22}$ J and the following boundary conditions: (A) $\psi_S = -38$ mV (constant ψ), $\psi_B = -55$ mV (constant ψ); (B) $\psi_S = -38$ mV (constant σ), $\psi_B = -47$ mV (constant ψ); (C) $\psi_S = -58$ mV (constant ψ), $\psi_B = -60$ mV (constant ψ); (D) $\psi_S = -58$ mV (constant σ), $\psi_B = -60$ mV (constant ψ). The parameters used to compute the best fit DLVO force profiles are also given in Table 3.

constant potential of −47 ± 5 mV and a streptavidin surface at a constant surface charge density of −0.01 mC/m^{-2} (−38 mV) (Table 3). Here the streptavidin surface charge density, not the potential, is constant, resulting in the increased double-layer repulsion at short separations. Surface interactions at constant charge density are more repulsive at short separations as one approaches the osmotic limit (Israelachvili, 1991; Hunter, 1985). Thus, the two bound charged biotin groups completely alter the electrostatic behavior (charge regulation) of the exposed streptavidin surface. At −38 mV, the streptavidin potential determined was lower than the −57 mV expected if each bound biotin imparts a negative charge to the surface. The calculated double-layer forces between fully inactivated streptavidin and biotin, assuming −1 unit charge/bound biotin, under both constant potential and constant charge boundary conditions are shown in Figure 10, curves C and D. Clearly, the potential of inactivated streptavidin is significantly less negative than expected. The surface potential of inactive streptavidin was also determined in measurements of the forces between two identical inactive streptavidin monolayers. In the latter case, the measured inactive streptavidin potential at pH 7.1 ± 0.1 was −15 ± 2 mV (Table 3, data not shown), which was also substantially lower than expected (see Discussion).

Effect of pH. The streptavidin p*I* is 6–6.5, and it was of interest to determine how the biotin–streptavidin forces change as the result of pH titration of the surface amino acids. The magnitude of the measured streptavidin surface potential at pH 6 was $|\Psi| = 29 \pm 5$ mV (Table 3; Helm et al., 1991). In previous measurements of the biotin–streptavidin interaction forces at pH 6 in 1 mM NaCl, no force was detected at $D > 4$ Å (Helm et al., 1991). A strong spring constant was utilized in the latter experiments, limiting measurement sensitivity. In order to detect weak forces between the two surfaces, we used a spring constant an order of magnitude weaker than that used in the previous work.

Figure 11 shows the force–distance curve for the interaction of streptavidin with a 5% biotin surface at pH 6 in phosphate buffer at 33 °C. The force profile is attractive at all separations under these conditions, and the onset of the measured attractive force occurs at $D = 500$ Å ($D_{BA} < 455$ Å). However, at $D < 160$ Å ($D_{BA} < 115$ Å), under the influence of the increased intersurface attraction, the surfaces rapidly jump into strong adhesive contact at $D = 45$ Å ($D_{BA} = 0$ Å). The attractive

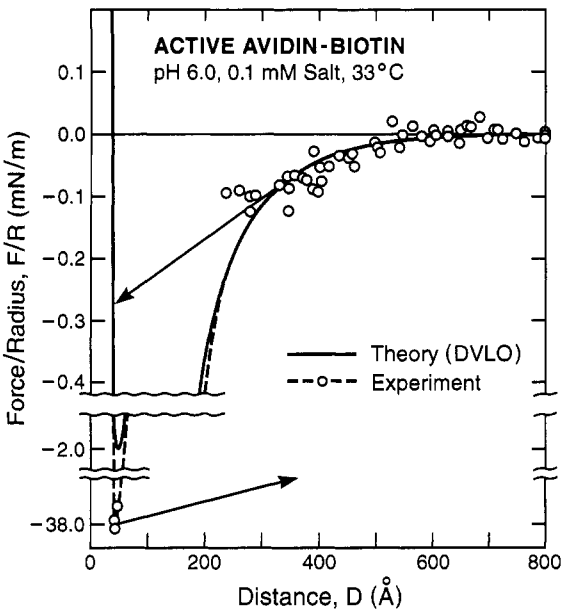

FIGURE 11: Force–distance profile between a streptavidin surface and a 5% biotin surface in 0.1 mM salt at pH 6.0 and 33 °C. The parameters used to compute the theoretical DLVO force profile (solid line through the data) are given in Table 3.

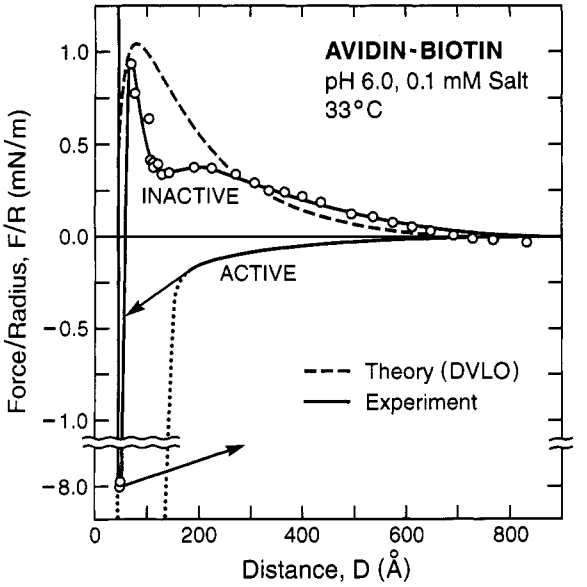

FIGURE 12: Force–distance profile between a streptavidin surface and a 5% biotin surface in 0.1 mM salt at pH 6.0 and 33 °C: active streptavidin (data of Figure 10), ···, partially inactivated streptavidin, o. The parameters used to compute the theoretical DLVO force profile are $\psi_S = -58$ mV (constant σ) and $\psi_B = -55$ mV (constant ψ).

force at $D = 45$ Å ($D_{BA} = 0$ Å) was 38 ± 4 mN/m, consistent with previous measurements, independent of pH (this work; Leckband et al., 1992; Helm et al., 1991).

The molecular origin of the measured force curve was determined from theoretical fits of the data to the superposition of the van der Waals and electrostatic forces. The theoretical curve in Figure 11 was obtained by calculation of the double layer force, with previously determined surface parameters of −55 and +29 mV (Table 3). The sign of the streptavidin potential was assumed. The agreement between the measured and calculated force curves is excellent, and none of the parameters were adjusted to obtain the theoretical curve. This agreement between the measured forces at $D > 150$ Å and the double-layer forces calculated on the basis of the independently measured streptavidin and biotin electrostatic surface parameters clearly demonstrates the absence of non-DLVO forces at $D > 150$ Å. Due to the jump into contact from *ca.* 150 Å, however, the forces governing the intermediate-range interactions could not be determined.

The electrostatic basis of the long-range attraction at $D >$ 150 Å and the absence of non-DLVO forces at $D < 150$ Å were verified by increasing the solution ionic strength to 10 mM with the 1:1 electrolyte $NaNO_3$ (data not shown). Under the latter conditions, there was no measured force between the surfaces at $D > 70$ Å ($D_{BA} > 25$ Å), and only the short-range nonequilibrium steric repulsive force was measured at smaller distances (*cf.* Figure 6). This is as expected since, in this experiment, the rate of approach exceeds the rearrangement rate, preventing the biotin and streptavidin molecules from aligning. These results show that only weak van der Waals and dominant double-layer forces govern the streptavidin–biotin interaction, as suggested by analysis of previous data at pH 7.2 and 0.1 mM salt (Figure 9).

Upon the addition of soluble biotin, both the long- and short-range attractive forces decreased correspondingly until the specific short-range attraction was abolished (Figure 12). The data in Figure 12 show partial streptavidin inactivation at pH 6.0 and demonstrate the correlation between the decreased adhesion and changes in the interaction forces. At pH 6.0, the entire force curve switches from purely attractive to repulsive, as binding of negatively charged biotin molecules reverses the streptavidin surface charge from net positive to net negative. This demonstrates conclusively that biotin binding increases the negative surface charge of streptavidin. The theoretical DLVO force calculated for fully charged inactivated streptavidin regulated by constant charge density is indicated in Figure 12. The negative deviation in the experimental data at $D < 200$ Å is attributed to an attractive force due to residual active streptavidin.

DISCUSSION

Interaction forces measured between two identical biotin–lipid surfaces are consistent with the DLVO theory of attractive van der Waals and repulsive electrostatic forces. The decay lengths of the double-layer electrostatic forces agree with theoretical predictions, and the degree of ionization increased with increasing pH and ionic strength, also as predicted by theory (Helm et al., 1986). In this work, the low surface charge densities are attributable to Na^+ binding (Claesson et al., 1989; Helm et al., 1986; Marra, 1986). Additionally, the low calculated surface ionizations may also be partially due to errors in the determination of the position of the outer Helmholtz plane. The presence of a Stern layer, arising from bound water or hydrated ions, introduces an uncertainty in the determination of the position of the plane of charge, resulting in underestimations of both the surface potential and the degree of ionization.

Calculations of the Hamaker constants between 5% biotin–lipid surfaces calculated from the adhesion force were somewhat higher than expected. Consequently, due to the substantial error in the estimation of ΔD, the initial calculated value of $A = 1 \times 10^{-20}$ J represents a lower bound. This anomalously large Hamaker constant indicates that attractive forces, other than the van der Waals force, likely operate between the 5% biotin bilayers. The source of this additional short-range attraction is likely due to interactions between the hydrophobic biotin headgroups. This is consistent with the observation that the measured Hamaker constant between 0.5% biotin bilayers is similar to other measurements (Marra & Israelachvili, 1985).

The measured force laws between identical streptavidin surfaces agree with DLVO theory and accurately account for the observed streptavidin aggregation behavior in solution. The interprotein attractive potential can be determined directly from the measured interprotein attractive force. The van der Waals energy between two spheres of radius r is given by (Israelachvili, 1991)

$$W = -Ar/6\Delta D \quad (8)$$

where A is the Hamaker constant and ΔD is distance of the adhesive minimum from the van der Waals plane of origin. Using the measured Hamaker constant, $A = 9.0 \times 10^{-21}$ J (Helm et al., 1991), an average streptavidin radius of $r = 26$ Å (Weber et al., 1992; Darst et al., 1991), and $\Delta D = 9$ Å (Helm et al., 1991), the calculated attractive energy between two streptavidin molecules is $W = 4.3 \times 10^{-21}$ J, or $\sim kT$. On the basis of these calculations, no aggregation is expected since $>10kT$ is required for the formation of stable aggregates (Hunter, 1989). Due to the weak attractive energy relative to kT, the extent of aggregation is expected to be small at pH 6 and 0.1 mM NaCl. Streptavidin can be crystallized from pure water and isopropyl alcohol (Green, 1975). However, these experiments demonstrate that electrostatic repulsion and hydrated Na^+ binding further increase streptavidin stability against aggregation by increasing the steric and electrostatic repulsive forces relative to attractive forces (Leckband et al., 1993; Claesson et al., 1990; Marra, 1986). Consequently, soluble streptavidin is predicted to be stable to aggregation at the higher pH, as is observed experimentally (Green, 1975).

Calculations of the hypothetical attractive force between interdigitated monolayers is slightly higher than those predicted on the basis of the attraction between the outer streptavidin surfaces (secondary minimum). This suggests the formation of closer, slightly more dehydrated, lateral interprotein contacts, which result in stronger van der Waals attraction. The magnitude of the interprotein attraction is consistent with the fact that streptavidin forms two-dimensional crystals when bound to biotin-functionalized monolayers at the air–water interface (Darst et al., 1991; Ahlers et al., 1990; Blankenburg, 1989). Additionally, despite the increased electrostatic repulsive barrier preceding interdigitation at pH 7.2, the magnitude of the attractive force at $D = 45$ Å (interdigitated streptavidin monolayer) is unchanged relative to that at pH 6. The results in Figures 3 and 4 indicate that the enhanced repulsive barrier at $D > 45$ Å should slow the crystallization rate at pH 7.2. However, at both pH values, the lateral protein attractive forces are sufficiently strong to promote crystal growth, in agreement with experiments (personal observations). Consequently, the measured interprotein force profiles account for the observed two-dimensional crystallization behavior of streptavidin. Similar studies with other proteins are expected to similarly aid predictions of their solution and interfacial behavior.

The measurements of streptavidin–biotin interaction forces at different pH and ionic strength together with fits of the data to theoretical force curves demonstrate that the equilibrium noncontact streptavidin–biotin interactions are mediated entirely by DLVO forces. At short separations, the immobilized protein–ligand interaction is also influenced by nonequilibrium steric forces. The molecular forces governing the noncontact biotin–streptavidin interaction were determined from fits of the data to a superposition of van der Waals and double-layer forces obtained from numerical solutions to the nonlinear Poisson–Boltzmann equation, for which boundary conditions were specified independently for both the biotin and streptavidin surfaces. The determined electrostatic surface parameters were within experimental error of independent measurements between identical surfaces (*e.g.*, biotin–biotin); hence, the streptavidin–biotin force laws could be predicted entirely from independently measured electrostatic streptavidin and biotin surface parameters without invoking non-DLVO forces or large molecular reorientations. The attenuation of long-range forces at high ionic strength further supports the electrostatic origin of the long-range forces at different pH values. Thus, in contrast to previous hypotheses regarding the molecular origins of the long-range forces (Leckband et al., 1992), these results show conclusively that the intermediate to long-range streptavidin–biotin interaction is governed entirely by electrostatic and van der Waals forces.

These results clearly demonstrate the impact of protein structure on noncontact interactions in molecular recognition. The latter interactions ultimately determine the rates of biological associations. Since the biotin surface charge is invariant over the pH range of interest (Table 3), the measured differences in the force curves at pH 6 and 7.2 (Figures 9 and 11) are attributed to the titration of surface amino acids. Of the positively and negatively charged amino acids exposed on the biotin binding surface, only the histidines ($pK = 6.2$) near each of the two biotin binding sites titrate in the 6.0–7.2 pH range. Furthermore, at pH 6.0 the net unit charge per streptavidin is +0.5, and a pH increase to 7.2 presumably titrates these exposed histidines, reversing the unit charge to –0.8/streptavidin. This small shift causes a dramatic change from a repulsive to a purely attractive force law. The consequence of this change would be a substantial enhancement in the binding rate at pH 6.0. Thus, if the altered surface potential is due to histidine titration, a change of only 0.6 unit of charge/histidine results in a substantial change in the overall interaction. This behavior is clearly linked to the amino acid composition of the streptavidin surface, directly demonstrating that protein interactions and their pH sensitivity depend directly on the detailed amino acid composition of protein surfaces.

The dramatic pH-dependent changes in intermolecular forces are most pronounced at low ionic strength. At high ionic strengths, the effects of the screened long-range electrostatic forces will only be felt within 20 Å of the protein surface, and in this system, that regime is dominated by a short-range nonequilibrium steric force. Moreover, at high ionic strengths, the distance between charges likely exceeds the Debye screening length, and the charge will be less delocalized; consequently, the forces experienced by an approaching ligand will be much more sensitive to the local protein structural details. Hence, the positively charged histidines near the biotin binding site will enhance ligand trajectories within a much reduced range of the streptavidin binding site.

Measured forces between active streptavidin and biotin (Figures 6 and 7) indicate a significant difference in the double-layer forces measured with 5% and 0.5% biotin surfaces. There are two potential effects that may cause the increase in intersurface repulsion at 0.5% coverage. First, the dissimilarity in the biotin surface and streptavidin surface potentials is more pronounced at 5% biotin, and this will lower the double-layer repulsive force. Second, the greater hydrophobicity of the 5% biotin surface would increase the intersurface attraction relative to the 0.5% surface, thereby lowering the apparent potential. Finally and most significantly, the intermediate-range double-layer force between identical 0.5% surfaces is more repulsive than that between 5% biotin surfaces. The

latter effect is due to the change in the charge regulation behavior from constant potential to constant charge at lower biotin densities (*cf.* Figures 1 and 2). Additionally, the degree of ionization is greater at the lower coverage (Table 1), consistent with theory (Helm et al., 1986). Together, all of these factors may result in increased streptavidin–biotin repulsion at 0.5% relative to the 5% biotin case.

The anomalously low electrostatic surface potential and altered charge regulation mechanism of biotin-inactivated streptavidin cannot be explained by the simple charge increase due to biotin binding. First, the boundary condition governing the streptavidin electrostatic surface behavior switched from constant potential to constant charge density (Hunter, 1985; Israelachvili, 1991). This behavior is attributed to the carboxylic acid groups of bound biotin, and it implies that single charged moieties can alter not only the protein surface charge but also the electrostatic boundary condition governing surface charge regulation. Constant potential boundary conditions describe the active streptavidin surface interactions, and they are typically assumed in calculations of electrostatic intermolecular potentials (Sharp et al., 1987b). Clearly, the validity of this assumption depends on the charged surface groups, and its improper use can result in substantial underestimations of the calculated protein–ligand repulsive potentials at short separations (*cf.* Figure 10, curve C).

Second, the determined inactive streptavidin surface potentials are clearly much lower than anticipated for complete biotin-dependent surface charging, which is indicative of possible structural changes in the protein monolayer. Streptavidin undergoes a conformational change upon biotin binding (Green, 1975), which could result in (i) changes in the charged amino acid composition of the exposed streptavidin surface or (ii) the ejection of bound negative counterions. The latter two events would alter the charge density of the exposed streptavidin surface, resulting in the low apparent surface potential. The biotin–streptavidin bond is also much more labile at interfaces than in solution (Spinke, 1992). Surface plasmon experiments indicate that as much as 20% of the biotin-bound streptavidin is displaced from the surface by 10^{-4} M biotin within 48 h (Spinke, 1992). Although the majority of inactivated streptavidin data was acquired within 12 h of biotin addition, loss of bound streptavidin would reduce the measured potential of the streptavidin-coated surface at the plane of protein contact. These two possibilities could not be distinguished on the basis of force measurements, and additional experimental evidence is needed to conclusively verify the basis of the observed behavior.

Protein structure purportedly significantly impacts ligand association dynamics. A reduction in the total intermolecular repulsion by intermolecular attractive forces will increase bimolecular association rates (Leckband et al., 1992; Berg & von Hippel, 1985). Protein structural forces purportedly enhance protein association rates by diffusional preorientation of the reactants (Creighton, 1989; Margoliash & Bosshard, 1983; Sharp et al., 1987a; Berg & von Hippel, 1985). The superoxide dismutase surface charge distribution is optimally controlled to enhance superoxide binding to the negatively charged protein. Likewise the charge and dipolar complementarity of cytochromes and their redox partners are tailored for optimal preorientation of binding trajectories (Northrup et al., 1987; Matthews et al., 1983). The results presented in this work are the first to directly quantify the range, magnitude, and environmental sensitivity of the forces arising directly from protein surface properties. Electrostatic interactions are likely the most significant forces governing protein association dynamics, whereas shorter ranged hydrogen bonds, salt bridges, van der Waals forces, and hydrophobic contacts compose the majority of the short-range forces determining tight binding (Stayton & Sligar, 1990). In these measurements, the amplitude of the long-range attractive force constitutes at most 10% of the total measured adhesive force, consistent with previous findings (Stayton & Sligar, 1990). Consequently, by lowering intermolecular repulsive potentials, the noncontact attractive forces likely enhance association rates, but do not necessarily constitute the majority of the binding force.

The effect of temperature on receptor-mediated intermembrane cohesive strength was attributed to altered membrane fluidity. The characteristics of the force profiles at $D > 60$ Å ($D_{BA} > 15$ Å) remained unchanged. As a result of the restricted surface mobilities at 25 °C, mismatches between streptavidin and biotin on opposing surfaces were not relieved. The number of intermembrane bonds, and hence the adhesion, was substantially reduced due to insufficient lateral mobility to permit the rearrangements that would lead to bond formation. The increased fluidity was therefore manifested as increased intermembrane adhesion. However, given sufficient time, the adhesion at 25 °C is expected to reach the same value as that at 33 °C as biotin continues to diffuse to and rearrange within the contact region.

Molecular rearrangements associated with the increased surface mobility were also apparent in the relaxation times of the intermediate-range repulsive steric force. The force is attributed to steric interactions between the unbound biotin headgroups and the streptavidin surface. When the surface mobility was reduced, a short-range steric force was always measured, indicating that the relaxation times were greater than the time scale of the measurements (*e.g.*, seconds to minutes). This behavior is similar to that reported previously (Leckband et al., 1992). However, these data demonstrate that these dynamic interactions are both characteristic of the streptavidin–biotin interaction and independent of other parameters, such as surface coverage or charge density. Furthermore, the correlation of the increased relaxation times of the rearrangements with the reduced adhesion confirms that the latter effect is due to the membrane fluidity and not to a temperature-dependent change in the bond energy.

Cell adhesion strength depends on the number of intermembrane bonds formed, as well as on the bond strength (Bell, 1988; Lauffenburger, 1990; Evans et al., 1991). In these experiments, ligand–receptor mismatches on opposing membranes reduced the number of intermembrane bonds formed. In all cell adhesion models, receptor and ligand diffusivities are essential parameters affecting the cell attachment strength (Wiegel, 1984; Bell, 1988). Membrane receptors exhibit diffusion coefficients of 10^{-9}–10^{-11} cm^2/s on actual fluid cell membranes (Barisas, 1984; Kapitza & Sackmann, 1980). In this work, the significant drop in the measured interbilayer adhesion following bilayer solidification directly illustrates the role of cell surface mobility in determining receptor-mediated intermembrane adhesive strength.

The expected 77% or 4-fold decrease in intermembrane adhesion following a 10-fold biotin surface dilution was calculated on the basis of an assumed streptavidin surface density of 5000 Å^2/molecule. The reported streptavidin areas range from 2350 to 3100 Å^2 (Weber et al., 1989; Hendrickson et al., 1989; Vaknin et al., 1991, 1993), and reported fractional occupied streptavidin areas on supported monolayers range from 0.52 to 0.66 (Schmitt et al., 1992; Darst et al., 1991).

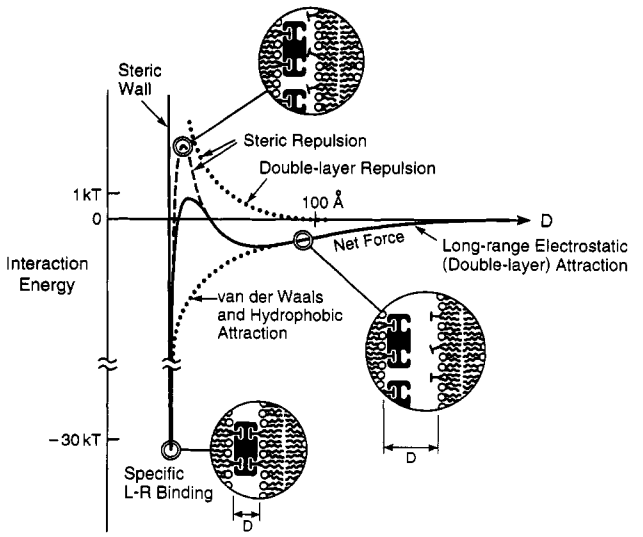

FIGURE 13: Schematic receptor–ligand interaction potential illustrating how four different types of interactions—electrostatic, van der Waals, hydrophobic, and steric—control the attractive and repulsive forces at different distance regimes from $D > 100$ Å down to $D \approx 5$ Å, below which site-specific binding forces take over. A complete description of the interaction would also have a time axis to illustrate the time dependence of the steric forces and lateral diffusion-controlled specific interactions.

On the basis of these values, the 10-fold decrease in biotin coverage should, nevertheless, result in a decrease of 77 ± 4%. At 25 and 33 °C, the measured decreases were 66% and 60%, respectively, corresponding to a factor of 2.5–3-fold less than the anticipated 77% reduction. The adhesive energy is assumed to depend on the local bond density in the adherent region (Lauffenburger, 1990; Evans et al., 1991; Bell, 1988). The observed effect is not entirely unexpected since the lateral diffusion of receptors and ligands into the contact area will increase the bond density (*i.e.*, the adhesion), and the maximum equlibrium adhesion energy is expected to be similar to that measured at 5% biotin coverage. Thus, the measured adhesion force at 0.5% coverage should be higher than the anticipated value, assuming no diffusion. Additionally, nonideal effects due to the large excluded streptavidin area will also result in increased adhesion. The large capture radius of streptavidin relative to the biotin headgroup area results in a higher binding probability, that is, greater adhesion. Conversely, intraplanar biotin aggregation, particularly at high surface densities, would reduce the biotin activity and lead to reduced bond formation; consequently, the measured adhesion at 5% biotin coverage may actually be too low, also accounting for the nonlinear dependence of adhesion force on ligand density. In summary, receptor-mediated intermembrane adhesion on these fluid bilayer surfaces may be affected by a number of factors, and the elucidation of such nonideality and time effects on local receptor density warrants further study.

The measurements presented in this work demonstrate the remarkable diversity of intermolecular forces available for the regulation of biological interactions. Nature has clearly evolved a vast array of biological control mechanisms, ranging from the genetic control of protein structure to the expression of steric carbohydrate barriers at the cell surface, for the simultaneous modulation of the time and distance dependencies of interaction forces. The most precise control is achieved in biological selectivity, which is governed by the precise tuning of intermolecular forces within protein binding sites. The detailed distance dependencies of recognition force laws ultimately dictate biological interaction potentials and resulting association rates (Figure 13). This diverse library of molecular forces can be remarkably fine-tuned over different distance regimes, from distances greater than 100 Å to intermolecular contact. Electrostatic interactions alone can result in a rich diversity of force profiles exhibiting both attractive and repulsive regimes, depending on the solution conditions, the relative potentials and signs, and the charge distributions. The van der Waals and hydrophobic forces can likewise be modulated by the exposed surface groups and exposed area, and the superposition of these forces on the already versatile electrostatic force results in a rich variety of behavior. The additional involvement of non-DLVO forces such as hydrophobic or short-range steric forces provides additional flexibility to precisely modulate short-range interactions. Furthermore, the measurements in this work demonstrate the extreme importance of time-dependent or nonequilibrium forces in the control of biological phenomena. Thus, transients near membrane surfaces and protein breathing add further temporal control of the interactions over both short and large separation distances. In summary, by controlling the magnitudes, signs, distance dependencies, and time-dependence of intermolecular force laws, biological systems can achieve the very precise timing and response required to control a multitude of interactions *in vivo*.

ACKNOWLEDGMENT

We thank J. Yanez and D. Pearson for their assistance with the light-scattering measurements and Robert Hill for his invaluable technical assistance.

REFERENCES

Adams, G., & Israelachvili, J. (1976) *J. Chem. Soc., Faraday Trans. 1, 74*, 975–1001.

Ahlers, M., Blankenburg, R., Grainger, D. W., Meller, P., Ringsdorf, H., & Salesse, C. (1990) *Thin Solid Films 180*, 93–98.

Allison, S. A., Ganti, G., & McCammon, J. A. (1985) *Biopolymers 24*, 1323–1336.

Baltz, J. M., & Cone, R. A. (1990) *J. Theor. Biol. 142*, 163–178.

Barisas, G. (1984) in *Cell Surface Dynamics* (Perelson, A., DeLisi, C., & Wiegel, F., Eds.) Marcel Dekker, Inc., New York.

Bayer, E., & Wilchek, M. (1990) *Methods Enzymol. 184*, 49–67.

Bell, G. (1988) *Physical Basis of Cell-Cell Adhesion*, CRC Press, Inc., Boca Raton, FL.

Berg, O., & von Hippel, P. (1985) *Annu. Rev. Biophys. Biophys. Chem. 14*, 131–160.

Blankenburg, R., Meller, P., Ringsdorf, H., & Salesse, C. (1989) *Biochemistry 28*, 8214–8221.

Bongrand, P., & Bell, G. (1984) in *Cell Surface Dynamics* (Perelson, A., DeLisi, C., & Wiegel, F., Eds.) Marcel Dekker, Inc., New York.

Cevc, G., & Marsh, D. (Eds.) (1987) *Phospholipid Bilayers: Physical Principles and Methods*, John Wiley and Sons, New York.

Chan, D., & Horn, R. G. (1986) *J. Chem. Phys. 83*, 5311–5324.

Chan, D., Healy, T. W., & White, L. R. (1981) *J. Chem. Soc., Faraday Trans. 1 72*, 2844–2865.

Chen, Y. L., Helm, C., & Israelachvili, J. (1991) *Langmuir 7*, 2694–2699.

Claesson, P., Carmona-Ribeiro, A. M., & Kurihara, K. (1989) *J. Chem. Phys. 93*, 917–922.

Claesson, P., Herder, P., Berg, J., & Christenson, H. (1990) *J. Colloid. Interface Sci. 136*, 541–551.

Creighton, T. E. (1989) *Proteins*, W. H. Freeman and Company, New York.

Darst, S., Ahlers, M., Meller, P., Kubalek, E., Blankenburg, R., Ribi, H., Ringsdorf, H., & Kornberg, R. (1991) *Biophys. J. 59*, 387–396.

Evans, E. (1985) *Biophys. J. 48*, 185–192.
Evans, E., Berk, D., & Leung, A. (1991) *Biophys. J. 59*, 838–848.
Grabbe, A. (1993) *Langmuir 9*, 797–801.
Green, M. (1975) *Adv. Protein Chem. 29*, 85–133.
Helm, C., Laxhuber, M., Lösche, M., & Möhwald, H. (1986) *Cell Polym. Sci. 264*, 46–55.
Helm, C., Knoll, W., & Israelachvili, J. (1991) *Proc. Natl. Acad. Sci. U.S.A. 88*, 8169–8173.
Hendrickson, W. A., Pähler, A., Smith, J., Satow, Y., Merritt, E. A., & Phizackerly, R. P. (1989) *Proc. Natl. Acad. Sci. U.S.A. 86*, 2190–2194.
Herron, J. M., Müller, W., Paudler, M., Riegler, H., Ringsdorf, H., & Suci, P. A. (1992) *Langmuir 8*, 1413–1416.
Hunter, R. J. (1989) *Foundations of Colloid Science*, Clarendon Press, Oxford, U.K.
Israelachvili, J. (1991) *Intermolecular and Surface Forces*, 2nd ed., John Wiley Intersciences, New York.
Israelachvili, J. (1992) *Surf. Sci. Rep. 14*, 109–160.
Israelachvili, J., & Pashley, R. (1982) *Nature 300*, 341–342.
Kapitza, H. G., & Sackmann, E. (1980) *Biochim. Biophys. Acta 595*, 56–64.
Koczak, R. E., & Subramaniam, S. (1993) *Protein Sci. 2*, 915–926.
Koppenol, W., & Margoliash, E. (1982) *J. Biol. Chem. 257*, 4426–4437.
Lauffenburger, D. (1991) *Annu. Rev. Biophys. Biophys. Chem. 20*, 387–414.
Leckband, D. E., Israelachvili, J., Schmitt, F.-J., & Knoll, W. (1992) *Science 255*, 1419–1421.
Leckband, D., Helm, C., & Israelachvili, J. (1993) *Biochemistry 32*, 1127–1140.
Margoliash, E., & Bosshard, H. R. (1983) *Trends Biochem. Sci. 8*, 316–320.
Marra, J. (1986) *J. Phys Chem. 90*, 2145–2150.
Marra, J., & Israelachvili, J. (1985) *Biochemistry 24*, 4608–4618.
Marra, J., & Israelachvili, J. (1986) *Methods Enzymol. 127*, 353–360.
Matthew, J. B., Weber, P. C., Salemme, F. R., & Richards, F. M. (1983) *Nature 301*, 169–171.
Metzler, D. E. (1977) *Biochemistry*, Academic Press, New York.
Northrup, S. H., Boles, J. O., & Reynolds, J. (1987) *J. Phys. Chem. 91*, 5991–5998.
Northrup, S. H., Boles, J. O., & Reynolds, J. (1988) *Science 241*, 67–70.
Roess, D. A., Niswender, G. D., & Barisas, B. G. (1988) *Endocrinology 122*, 261–269.
Ryan, T. A., Myers, J., Holowka, D., Bard, B., & Webb, W. W. (1988) *Science 239*, 61–64.
Schmitt, F.-J. (1991) Ph.D. Thesis, University of Mainz, Mainz, Germany.
Schmitt, F.-J., Blankenburg, R., Häussling, L., Ringsdorf, H., Weisenhorn, A. L., Hansma, P. K., Leckband, D. E., Israelachvili, J., & Knoll, W. (1992) in *Microstructures in Biological Research* (Schnur, J. M., & Peckerar, M., Eds.), Plenum Press, New York.
Sharp, K., Fine, R., & Honig, B. (1987a) *Science 236*, 1460–1463.
Sharp, K., Rine, R., Schulten, K., & Honig, B. (1987b) *J. Phys. Chem. 91*, 3624–3631.
Stayton, P., & Sligar, S. (1990) *Biochemistry 29*, 7381–7386.
Spinke, J., (1992) Ph.D. Thesis, University of Mainz, Mainz, Germany.
Torney, D. C., Dembo, M., & Bell, G. (1986) *Biophys. J. 49*, 501–507.
Vaknin, D., Als-Nielsen, J., Piepenstock, M., & Lösche, M. (1991) *Biophys. J. 60*, 1545–1552.
Vaknin, D., Kjaer, K., Ringsdorf, H., Blankenburg, R., Piepenstock, M., Diederich, A., & Lösche, M. (1993) *Langmuir 9*, 1171–1174.
Weber, P. C., Ohlendorf, D. H., Wendoloski, J. J., & Salemme, F. R. (1989) *Science 243*, 3239–3241.
Weber, P. C., Wendolowski, J. J., Pantoliano, M. W., & Salemme, F. R. (1992) *J. Am. Chem. Soc. 114*, 3197–3200.
Wendolowski, J. J., Matthew, J., Weber, P. C., & Salemme, F. R. (1987) *Science 238*, 794–797.
Wiegel, F. W. (1984) in *Cell Surface Dynamics* (Perelson, A., DeLisi, C., & Wiegel, F., Eds.) Marcel Dekker, Inc., New York.